

Explore-Before-Talk: Multichannel Selection Diversity for Uplink Transmissions in Machine-Type Communication

Jinho Choi, Jihong Park, and Shiva Pokhrel

Abstract: Improving the data rate of machine-type communication (MTC) is essential in supporting emerging Internet of things (IoT) applications ranging from real-time surveillance to edge machine learning. To this end, in this paper we propose a resource allocation approach for uplink transmissions within a random access procedure in MTC by exploiting multichannel selection diversity, coined *explore-before-talk (EBT)*. Each user in EBT first sends pilot signals through multiple channels that are initially allocated by a base station (BS) for exploration, and then the BS informs a subset of initially allocated channels that are associated with high signal-to-noise ratios (SNRs) for data packet transmission by the user while releasing the rest of the channels for other users. Consequently, EBT exploits a multichannel selection diversity gain during data packet transmission, at the cost of exploration during pilot transmission. We optimize this exploration-exploitation trade-off, by deriving closed-form mean data rate and resource outage probability expressions. Numerical results corroborate that EBT achieves a higher mean data rate while satisfying the same outage constraint, compared to a conventional MTC protocol without exploration.

Index Terms: Machine-type communication, multichannel selection diversity, resource allocation, uplink transmission

I. INTRODUCTION

THE Internet of things (IoT) has sparked the upsurge in uplink machine-type communication (MTC) traffic [1], [2]. The conventional wireless systems postulate their sporadic traffic with small payload size (e.g., thermometers, barometers) [3]. However, emerging IoT applications are envisaged to require higher MTC transmission rates. For instance, e-health wearables generate time-series data. Real-time surveillance cameras report video frames. Furthermore, edge learning devices exchange on-device machine learning models, some of which comprise millions of model parameters [4].

In MTC, random access approaches are considered to support a number of MTC devices. In particular, 4-step random access procedure is considered in [5]. In the first step, devices or MTC user equipment (UE) is to randomly choose a preamble within

a pool of preambles (that is to be shared with all UEs). After the response from a base station (BS) in the second step, the UEs can transmit their data packets through allocated channels to the BS in the third step. In this paper we propose a resource allocation approach for uplink transmissions in the third step, termed *explore-before-talk (EBT)*. As illustrated in Fig. 1(b), at the first phase of EBT, every MTC UE sends pilot signals through $W (\geq 1)$ channels that are initially allocated by the BS for exploration, and then the BS informs a subset of initially allocated channels that are associated with high signal-to-noise ratios (SNRs), say \bar{W} channels of highest SNRs, where $\bar{W} \leq W$, for data packet transmission by the UE while releasing the rest of the channels for other UEs. Then, at the second data packet transmission phase, each UE uploads data only using \bar{W} highest SNR channels.

Compared to a conventional approach whose $W = \bar{W}$ (i.e., no exploration) as depicted in Fig. 1(a), EBT exploits a *multichannel selection diversity* gain during the data transmission phase, at the cost of the channel exploration during the pilot transmission phase. To illustrate this, consider an example with three unit-bandwidth channels, in which one good channel provides the unity spectral efficiency, while the other two poor channels have ignorable spectral efficiencies. In the conventional approach with $\bar{W} = W = 1$, a single channel is uniformly randomly selected, and therefore the mean data rate is $1/3$. By contrast, in EBT with $W = 3$ and $\bar{W} = 1$, the mean data rate achieves 1 by selecting the best channel after exploration. With less exploration, $W = 2$, the mean data rate decreases to $2/3$, showing the trade-off between the exploring bandwidth and the data rate at exploitation.

Focusing on this exploration-exploitation trade-off, we aim to answer the question whether EBT achieves higher data rate, by fairly comparing the conventional method and EBT under a common traffic model and a resource outage requirement.

Related Works. To improve the uplink performance of MTC, random access techniques have been studied, such as device grouping methods [6], coded random access [7], non-orthogonal multiple access (NOMA) [8], and sparse code multiple access (SCMA) [9]. While the variety of works have addressed reducing random access collision, improving MTC data rates has recently attracted much attention from both academia and industry, towards supporting emerging applications categorized as broadband IoT [10]. Next, in terms of the exploring operations before exploitation, this work has been partly inspired by listen-before-talk (LBT) in dynamic spectrum access (DSA), in which secondary users sense the channel before transmission,

Manuscript received October 27, 2020; approved for publication October 27, 2020. This paper is specially handled by EIC and Division Editor with the help of three anonymous reviewers in a fast manner.

This research was supported by the Australian Government through the Australian Research Council's Discovery Projects funding scheme (DP200100391).

J. Choi, J. Park, and S. Pokhrel are with the School of Information Technology, Deakin University, Geelong, VIC 3220, Australia, email: {jinho.choi, jihong.park, shiva.pokhrel}@deakin.edu.au.

J. Choi is the corresponding author.

Digital Object Identifier: 10.1109/JCN.2020.000029

1229-2370/19/\$10.00 © 2020 KICS

Creative Commons Attribution-NonCommercial (CC BY-NC).

This is an Open Access article distributed under the terms of Creative Commons Attribution Non-Commercial License (<http://creativecommons.org/licenses/by-nc/3.0>) which permits unrestricted non-commercial use, distribution, and reproduction in any medium, provided that the original work is properly cited.

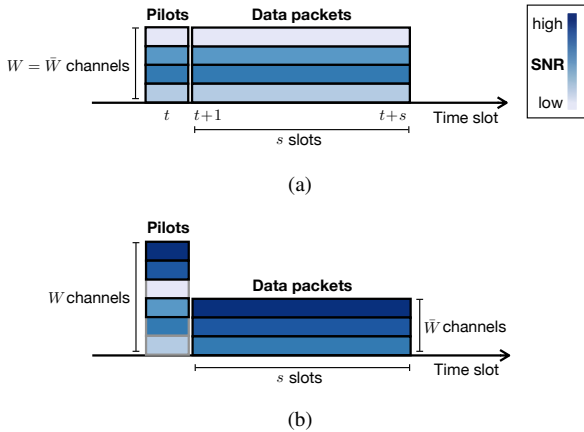


Fig. 1. An illustration of (b) EBT exploiting a multichannel selection diversity gain during s slots, obtained from the exploration at slot t , compared to (a) a conventional MTC uplink allocation without exploration: (a) Conventional ($W = \bar{W}$) and (b) EBT ($W > \bar{W}$).

in order to avoid the channels occupied by primary users [11]. A resource allocation method for MTC is discussed in [12] to improve the energy efficiency by taking into account the SNR or channel quality indicator (CQI). In our proposed EBT, MTC users explore the channels providing the highest SNRs for data transmission, which is similar to that in [12]. However, we consider multiple channels per MTC user to exploit selection diversity as illustrated in Fig. 1 (while in [12], one channel per MTC user is considered). Lastly, ordered selection rules have been applied in various applications. In [13] channel inversion power control is performed in the order of SNR to improve energy efficiency in uplink NOMA. In [14], interfering signals are canceled in order of their eigenvalues, thereby efficiently utilizing the multi-antenna degrees of freedom. In EBT, data transmission channels are selected in order of SNR for maximizing the data rates under limited bandwidth.

It is noteworthy that the proposed approach is suitable for MTC UEs with a number of data packets for uplink transmissions, e.g., data packets to exchange machine-learning models [4]. On the other hand, there would be a large number of MTC UEs that have short messages. For them, 2-step random access approaches are preferable [15]–[18].

Contributions and Organization. The contributions of this paper can be summarized as follows.

- We propose a resource allocation approach based on multichannel selection diversity in MTC, i.e., EBT, and derive its data rate in closed-form for given W and \bar{W} (see **Proposition 1**) to see the performance gain by selection diversity.
- We provide the optimality condition of \bar{W} guaranteeing a target outage probability in an overall system is provided (see **Proposition 2**), thereby proposing an algorithm that finds the optimal \bar{W} for a given W (see **Algorithm 1**).
- Numerical evaluations corroborate that EBT achieves higher mean transmission rate with less bandwidth while abiding by the same outage constraint compared to the conventional method.

The rest of the paper is organized as follows. In Section II, the system model for EBT is presented. In Section III, the mean

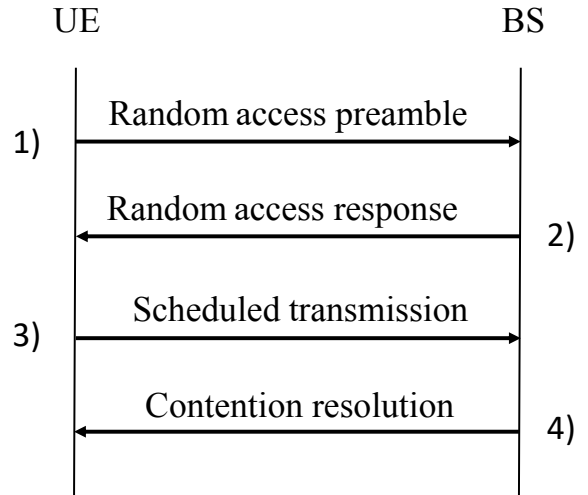


Fig. 2. 4-step random access procedure in MTC.

data rate is studied. In Section IV, the exploration and exploitation (i.e., W and \bar{W}) are optimized for a given outage requirement, which is validated by numerical evaluations in Section IV, followed by our conclusion in Section V.

II. SYSTEM MODEL

In this section, we present the system model to study resource allocation for uplink in MTC with multiple UEs and a BS.

Suppose that uplink transmissions are carried out based on 4-step random access procedure [3], [19], which is illustrated in Fig. 2. The first step is random access to establish connection to the BS with a pool of preambles consisting of L sequences. In the first step, an active UE transmits a randomly selected preamble through physical random access channel (PRACH). In the second step, the BS detects the transmitted preambles and sends responses. Once an active UE is connected to the BS, it can transmit data packets in the third step through dedicated resource blocks (RBs) or channels¹, which are physical uplink shared channel (PUSCH).

In this paper, we focus on the third step with preamble detection carried out in the first step as in [20]. Thus, it is assumed that the UEs without preamble collision can move to the third step, while the UEs with preamble collision would be backlogged. Note that in this case, the fourth step can be absorbed into the second step. As shown in Fig. 3, at slot t , there are $K(t)$ active UEs that transmit preambles. Among the $K(t)$ UEs in the first step, $Z(t)$ UEs are admitted for uplink transmissions in the third step. Here, $Z(t) \leq K(t)$ due to preamble collisions. Thus, every time slot t , it is necessary to allocate RBs to $Z(t)$ newly admitted UEs (without preamble collision) for uplink transmissions (in the third step). It is assumed that each newly admitted UE needs $s + 1$ slots for uplink transmissions. As will be explained later, the first slot is used to transmit a pilot signal to allow the BS to estimate the UE's channel in PUSCH. In addition, s can vary from one UE to another as will be considered in

¹We will use the terms resource block and channel interchangeably.

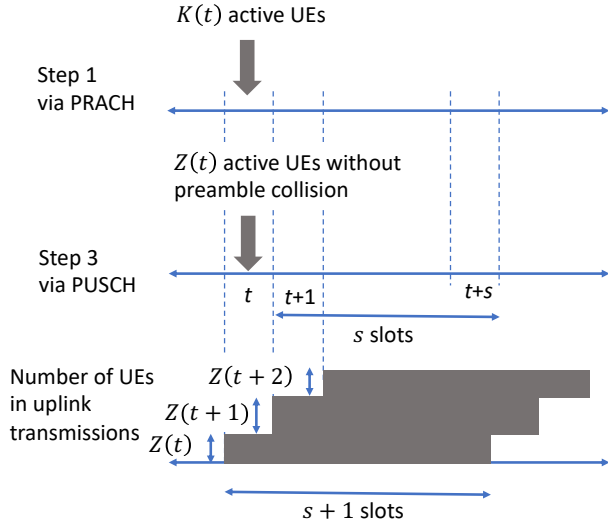


Fig. 3. 4-step random access procedure in MTC.

Section IV.

Suppose that there are N radio RBs for the UEs in the third step, i.e., uplink transmissions. Let $h_{n,k}$ denote the channel coefficient of the n th channel from UE k to the BS. Note that the newly admitted UEs in the third step transmit their signals through PUSCH, which is different from PRACH. Thus, the channel state information (CSI) estimation in the first step with preamble transmission does not provide the estimates of the $h_{n,k}$'s (which are the channel coefficients the RBs of PUSCH). This means that a newly admitted UE in the third step needs to transmit pilot signals together with data packets over s slots as illustrated in Fig. 1 to allow the BS to estimate $h_{n,k}$. Thus, for each UE in the third step, a total of $1 + s$ slots are required. For convenience, let $\gamma_{n,k} = |h_{n,k}|^2/\sigma^2$ be the signal-to-noise ratio (SNR) of the n th channel from UE k to the BS, where σ^2 is the noise variance.

With known CSI of all the UEs in the third step, the BS can perform optimal channel allocation with N RBs. For example, suppose that $N = 1000$ and each UE needs to have 10 RBs for uplink transmissions. Then, there can be up to 100 UEs that are connected simultaneously. In this case, in order to allocate 10 RBs for each UE, the CSI estimation of all $N = 1000$ channels per UE is required, which may require excessive pilot signaling. In addition, since the optimal channel allocation has to be updated when a set of new UEs join in every slot, it requires not only a high computational complexity, but also existing UEs to change their channels for uploading in every slot.

To avoid the difficulties stated above, a random subset of available channels can be simply allocated to a new admitted UE for uplink transmissions in the third step, which is regarded as a conventional approach.

III. MULTICHANNEL SELECTION DIVERSITY GAIN IN MEAN DATA RATE

In this section, we mainly focus on the performance gain of each UE in the third step by EBT, which can exploit multichannel selection diversity, in terms of the mean rate for given W ,

\bar{W} , and s as in Fig. 1. To understand the overall performance, it is also necessary to find the number of UEs in the third step for given N , which will be studied in Section IV.

Suppose that the BS randomly chooses W channels and allocates them to a new UE, say UE k . For convenience, let $\mathcal{W} = \{1, \dots, W\}$ be the index set of the allocated W channels. Note that since \mathcal{W} is a set of randomly selected channels from $\mathcal{N} = \{1, \dots, N\}$ as mentioned earlier, \mathcal{W} can be any subset of \mathcal{N} . Then, UE k transmits pilot signals through the W channels so that the BS can estimate their SNRs. The \bar{W} best channels among W in terms of SNR are selected and their indices are fed back to UE k so that the UE can transmit their data packets through the selected \bar{W} channels as shown in Fig. 1, where s represents the number of slots UE k sends packets. In doing so, EBT can exploit the multichannel selection diversity gain to increase the transmission rate, where W and \bar{W} are referred to as the number of the channels for exploration (to select the best \bar{W} channels) and exploitation (to transmit data packets), respectively.

In MTC, since UEs may have short messages to transmit and their mobility is limited, throughout the paper, it is assumed that *i)* each UE transmits packets over a finite number of slots, i.e., s is finite; *ii)* the channel coefficients remain unchanged for s slots.

For convenience, we omit the index of UE k in the rest of this section. Let

$$\gamma_{(W)} \geq \dots \geq \gamma_{(\bar{W}+1)} \geq \gamma_{(\bar{W})} \geq \dots \geq \gamma_{(1)}, \quad (1)$$

where $\gamma_{(w)}$ represents the w th lowest element. Then, for given $\{\gamma_w\}$, the $\gamma_{(w)}$'s are order statistics [21]. Since the UE will keep the channels of the \bar{W} highest SNRs, the mean transmission rate (in bits per second per Hz) per slot becomes

$$\begin{aligned} R(W, \bar{W}) &= \mathbb{E} \left[\sum_{i=W-\bar{W}+1}^W \log_2(1 + \gamma_{(i)}) \right] \\ &= \sum_{i=W-\bar{W}+1}^W \mathbb{E}[\log_2(1 + \gamma_{(i)})]. \end{aligned} \quad (2)$$

In (2), we assume that the transmission rate of each selected channel is set to its achievable rate (i.e., the channel capacity [22]).

For comparisons, consider a conventional approach where W_c channels are randomly allocated to a UE regardless of their SNRs. This can be seen as a special case of EBT with $W = \bar{W} = W_c$. Due to the random selection of W_c channels, it can be assumed that γ_w , $w \in \mathcal{W}_c = \{1, \dots, W_c\}$, is independent. Furthermore, for tractable analysis, we assume that γ_w is independent and identically distributed (iid). In this case, the mean transmission rate of the conventional approach becomes

$$R_c = W_c \mathbb{E}[\log_2(1 + \gamma_w)]. \quad (3)$$

For example, suppose that the UE has the SNR of channel $w \in \mathcal{W}$ that is distributed as follows:

$$f(\gamma_w) = \frac{1}{\bar{\gamma}} \exp\left(-\frac{\gamma_w}{\bar{\gamma}}\right), \quad \gamma_w > 0, \quad (4)$$

where $\bar{\gamma}$ is the mean SNR. That is, each channel is modeled as an independent and identical Rayleigh² fading channel and γ_w , $w \in \mathcal{W}$, is seen as a realization from the distribution in (4). Then, from [23], we have

$$R_c = W_c \frac{e^{\frac{1}{\bar{\gamma}}}}{\ln 2} E_1 \left(\frac{1}{\bar{\gamma}} \right), \quad (5)$$

where $E_n(x) = \int_1^\infty e^{-xt}/t^n dt$ is the exponential integral function of order n .

In a similar way, we derive the mean transmission rate of EBT in closed-form in the following lemma.

Lemma 1: For independent Rayleigh fading in (4), the mean transmission rate (per slot) of EBT is given as:

$$R(W, \bar{W}) = \sum_{w=W-\bar{W}+1}^W \frac{W!}{(W-w)!} \times \sum_{m=0}^{w-1} \frac{(-1)^m}{(w-1-m)!m!} \frac{e^{-\frac{a_{m,w}}{\bar{\gamma}}}}{a_{m,w} \ln 2} E_1 \left(\frac{a_{m,w}}{\bar{\gamma}} \right) \quad (6)$$

where $a_{m,w} = W - w + 1 + m$.

Proof: From (2), it can be shown that

$$R(W, \bar{W}) = \sum_{w=W-\bar{W}+1}^W \int_0^\infty \log_2(1 + \bar{\gamma}x) f_{(w)}(x) dx, \quad (7)$$

where

$$f_{(w)}(x) = \frac{W!}{(w-1)!(W-w)!} (1-e^{-x})^{w-1} e^{-(W-w+1)x}, \quad (8)$$

which is the probability density function (pdf) of the w th order statistic [21]. Applying the binomial expansion to (8), we obtain

$$f_{(w)}(x) = \frac{W!}{(w-1)!(W-w)!} \sum_{m=0}^{w-1} \binom{w-1}{m} (-1)^m e^{-a_{m,w}x}. \quad (9)$$

Plugging this into (7) completes the proof. \square

Next, for a large W , we can further simplify the mean transmission rate of EBT as follows.

Proposition 1: For independent Rayleigh fading in (4) with $W \gg \bar{W} \gg 1$, the mean transmission rate of EBT is:

$$R(W, \bar{W}) \approx \sum_{i=1}^{\bar{W}} \log_2 \left(1 + \bar{\gamma} \ln \frac{W}{i} \right). \quad (10)$$

Proof: For $W \gg \bar{W} \gg 1$, the w th highest SNR γ_w with $w \leq \bar{W}$ is large with a high probability. In this regime, the expectation of the logarithmic function increasing with diminishing returns in (2) is approximated as

$$\mathbb{E}[\log_2(1 + \gamma_w)] \approx \log_2(1 + \mathbb{E}[\gamma_w]). \quad (11)$$

²Other fading channels can be considered for γ_w , while we consider Rayleigh fading in this section as an example to demonstrate the gain from selection diversity in the third step. It is also assumed that power control is used to compensate large-scale fading. As a result, all W channels have the same mean SNR.

Next, we focus on $\mathbb{E}[\gamma_w]$ in (11). Let $F(\gamma)$ denote the probability that $\gamma_w \leq \gamma$. This cumulative distribution function (cdf) of the SNR is given by integrating its pdf in (8). For independent Rayleigh fading channels, following [21], the cdf is bounded as

$$\frac{w}{W+1} \leq F(\mathbb{E}[\gamma_w]) \leq \frac{w}{W}. \quad (12)$$

Therefore, for $W \gg 1$ we obtain

$$F(\mathbb{E}[\gamma_w]) \approx \frac{w}{W}. \quad (13)$$

Since $F(\gamma)$ is monotonically increasing, we can take the inverse function, yielding

$$\begin{aligned} \mathbb{E}[\gamma_w] &\approx F^{-1} \left(\frac{w}{W} \right) \\ &= \bar{\gamma} \ln \left(\frac{W}{W-w} \right). \end{aligned} \quad (14)$$

The last equality follows from the quantile function $F^{-1}(p)$ of the SNR distribution in (4) with $p = w/W \in [0, 1]$. Applying (14) with (11) to (2) and inverting the order of the summation finalize the proof. \square

In (10), considering the summation of the smallest values, i.e., $i = \bar{W}$, yields the following corollary.

Corollary 1: For independent Rayleigh fading in (4) with $W \gg \bar{W} \gg 1$, the mean transmission rate of EBT is lower bounded as:

$$R(W, \bar{W}) \geq \bar{W} \log_2 \left(1 + \bar{\gamma} \ln \frac{W}{\bar{W}} \right). \quad (15)$$

In (15), we can clearly see the gain from the multichannel selection diversity as the approximate rate increases with W when \bar{W} is fixed. In particular, we can see that the SNR term in the logarithm is effectively increased by a factor of $\ln(W/\bar{W})$.

For a fair comparison between the conventional and proposed approaches, the number of channels of the conventional approach is decided as

$$W_c = \frac{W + s\bar{W}}{1 + s}, \quad (16)$$

so that the total number of channels is the same as that of EBT, which is $W + s\bar{W}$. In Fig. 4, under the assumption of independent Rayleigh fading in (4), the mean transmission rates (per slot) as functions of W when $\bar{W} = 5$, $s = 10$, and $\bar{\gamma} = 10$ dB are shown for the conventional and proposed approaches. Note that in the conventional approach, W_c is decided as in (16) for given \bar{W} and W . The approximate mean transmission rate of EBT is given by (15) (shown by the solid line with cross markers). Clearly, for a fixed \bar{W} , a higher selection diversity gain can be achieved as W increases in EBT, i.e., the number of channels for exploration increases, there is a higher chance to choose the better \bar{W} channels for exploitation, which results in a higher mean transmission rate than that of the conventional one as shown in Fig. 4. Note that the mean transmission rate of the conventional approach also increases with W as W_c increases with W .

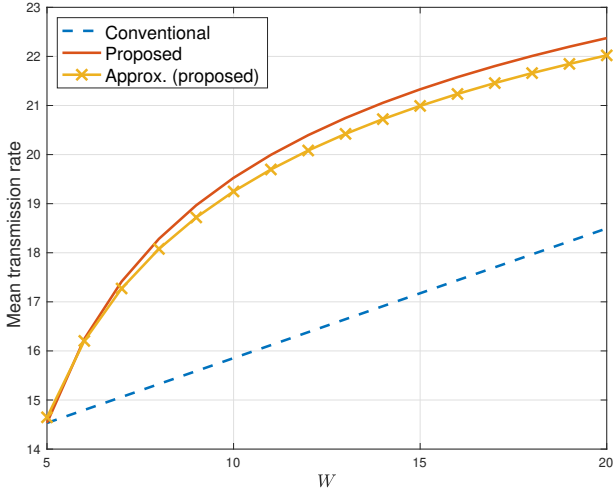


Fig. 4. Mean transmission rate (per slot) as functions of W when $\bar{W} = 5$, $s = 10$, and $\bar{\gamma} = 10$ dB.

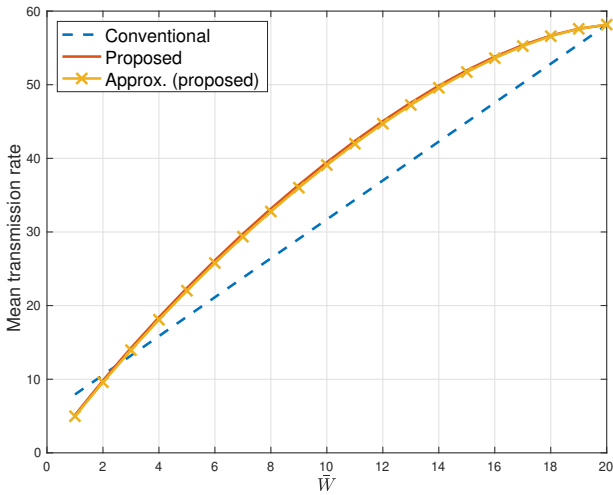


Fig. 5. Mean transmission rates (per slot) as functions of \bar{W} when $W = 20$, $s = 10$, and $\bar{\gamma} = 10$ dB.

In Fig. 5, the mean transmission rates as functions of \bar{W} when $W = 20$, $s = 10$, and $\bar{\gamma} = 10$ dB are shown for the conventional and proposed approaches. It is interesting to see that the conventional approach has a better performance when the number of channels for exploitation is small, e.g., $\bar{W} \leq 2$. In particular, when $\bar{W} = 1$ in EBT, W_c in the conventional approach becomes 2.727. Thus, although the multichannel selection diversity gain can help improve the transmission rate of EBT, a large number of channels for exploitation is still necessary for a higher transmission rate. It is also noteworthy that when $W = \bar{W} = W_c = 20$, EBT becomes the conventional approach, which results in the same mean transmission rate.

IV. EXPLORATION-EXPLOITATION OPTIMIZATION UNDER AN OUTAGE CONSTRAINT

As shown in Figs. 4 and 5, if the numbers of the channels for exploration and exploitation (i.e., W and \bar{W} , respectively) are well chosen, EBT can provide a higher transmission rate

than the conventional approach subject to (16). However, from a multiuser system point of view, for a fair comparison, we also need to consider the number of UEs in the third step for a given number of RBs, N . To this end, in this section, we consider the overall uplink system that includes the first and third³ steps, which is illustrated in Fig. 3.

The numbers of UEs in the first and third steps are random variables. As a result, although a new UE without preamble collision can move to the third step, it may not have a sufficient number of channels for uplink transmissions. This event is referred to as the outage event. The system has to be designed to keep the outage probability low or the outage probability less than e^{-d} , $d > 0$, is a design parameter. Thus, in this section, we first obtain an upper-bound on the outage probability and then consider an optimization problem formulation for a fair comparison between EBT and the conventional approach in terms of the mean transmission rate and outage probability.

A. Outage Probability

This subsection focuses on the outage event at a certain time, when the total N channels are exceeded by the allocated channels Q to newly admitted UEs as well as the remaining UEs who are previously admitted. For mathematical amenability, we consider the following assumptions in the outage probability analysis.

A1) Recall that $K(t)$ is the number of new UEs that send preambles to upload their data to the BS in slot t , where $K(t)$ is Poisson-distributed, i.e.,

$$K(t) \sim \text{Pois}(\lambda), \quad (17)$$

where λ is the mean of the number of new active UEs per slot. In addition, $K(t)$ is independent for every t .

A2) An admitted UE transmits its data over a number of slots and the number of slots required for each device to upload its data varies from one UE to another. Let ν_s denote the probability that a UE requires s slots to upload its data. In addition, assume that s_{\max} is the maximum number of slots to upload data from any UE. Thus, we have $\sum_{s=1}^{s_{\max}} \nu_s = 1$.

Recall that $Z(t)$ is the number of the admitted UEs (into the 3rd step), which are the UEs without preamble collisions, and $C_l(t)$ the number of active UEs that choose the l th preamble out of L preambles. Provided that an active UE chooses a preamble uniformly at random, under **A1**, we can show that

$$Z(t) = \sum_{l=1}^L \mathbb{1}(C_l(t) = 1), \quad (18)$$

where

$$C_l(t) \sim \text{Pois}\left(\frac{\lambda}{L}\right). \quad (19)$$

Thus, we can see that $Z(t)$ has the binomial distribution with parameter L and p , denoted by $\text{Bin}(L, p)$, or

$$\Pr(Z(t) = a) = \binom{L}{a} p^a (1-p)^{L-a}, \quad (20)$$

³In 4-step random access procedure, the second and fourth steps are for downlink, which will be ignored for the uplink performance analysis.

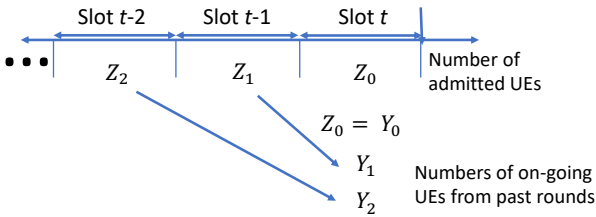


Fig. 6. The relationship between Z_s and Y_s .

where $p = (\lambda/L)e^{-(\lambda/L)}$. The Poisson approximation can be used for $Z(t)$, which results in the following distribution for $Z(t)$:

$$Z(t) \sim \text{Pois}\left(\lambda e^{-\frac{\lambda}{L}}\right). \quad (21)$$

For convenience, let $Z_0 = Z(t)$, and at time slot t , let Z_s be the number of the UEs that are admitted in the last s slot. Then, Z_s has the same distribution of Z_0 . In addition, let Y_s be the number of the UEs that still upload data among Z_s . Fig. 6 depicts the relationship between Z_s and Y_s . It is clear that $Y_0 = Z_0$ and Y_s might decrease with s (as more UEs likely finish their uploading as s increases). For $s \geq 1$, under **A2** with the Poisson approximation in (21), a fraction $\sum_{i=s}^{s_{\max}} \nu_i$ of Z_s remains at time t , leading to

$$Y_s \sim \text{Pois}(\lambda_s), \quad s = 1, \dots, s_{\max}, \quad (22)$$

where $\lambda_s = \lambda e^{-(\lambda/L)} \sum_{i=s}^{s_{\max}} \nu_i$.

Finally, using Y_s , we can express the number of allocated channels at a certain time slot as follows:

$$\begin{aligned} Q &= WY_0 + \sum_{s=1}^{s_{\max}} \bar{W}Y_s \\ &= WY_0 + \bar{W}V, \end{aligned} \quad (23)$$

where $V = \sum_{s=1}^{s_{\max}} Y_s$. Then, using the Chernoff bound [24], an upper-bound on the outage probability becomes

$$\begin{aligned} \Pr(Q > N) &\leq \mathbb{E}[e^{\theta(Q-N)}] \\ &= e^{-\theta N} \mathbb{E}[e^{\theta(WY_0 + \bar{W}V)}], \quad \theta \geq 0. \end{aligned} \quad (24)$$

It can also be shown that

$$\log \Pr(Q > N) \leq \psi(\theta; W, \bar{W}), \quad (25)$$

where

$$\psi(\theta; W, \bar{W}) = M_y(W\theta) + M_v(\bar{W}\theta) - \theta N. \quad (26)$$

The terms $M_y(\theta) = \log \mathbb{E}[e^{\theta Y_0}]$ and $M_v(\theta) = \log \mathbb{E}[e^{\theta V}]$ are the logarithmic moment generating functions (LMGFs) of Y_0 and V , respectively. An upper bound on the outage probability is given by

$$\begin{aligned} \Pr(Q > N) &\leq \min_{\theta \geq 0} \exp(\psi(\theta; W, \bar{W})) \\ &= \exp\left(\min_{\theta \geq 0} \psi(\theta; W, \bar{W})\right). \end{aligned} \quad (27)$$

It is well-known that the LMGF is convex (e.g., [25]). Thus, there exists a unique solution to the minimization on the right-hand side (RHS) in (27). We can also have the following monotonic property of $\psi(\cdot)$.

Lemma 2: For $\bar{W}' < \bar{W}'' \leq W$, it satisfies

$$\min_{\theta \geq 0} \psi(\theta; W, \bar{W}') \leq \min_{\theta \geq 0} \psi(\theta; W, \bar{W}''). \quad (28)$$

Proof: Let $\psi_1(\theta) = \psi(\theta; W, \bar{W}')$ and $\psi_2(\theta) = \psi(\theta; W, \bar{W}'')$. Since $\bar{W}' < \bar{W}''$, we have

$$\psi_2(\theta) - \psi_1(\theta) = M_v(\bar{W}''\theta) - M_v(\bar{W}'\theta) = \ln \frac{\mathbb{E}[e^{\bar{W}''\theta V}]}{\mathbb{E}[e^{\bar{W}'\theta V}]} \geq 0$$

or $\psi_1(\theta) \leq \psi_2(\theta)$, $\theta \geq 0$. Let $\theta^* = \arg\min_{\theta \geq 0} \psi_2(\theta)$. Note that since the LMGF is convex, θ^* exists. Then, we have

$$\min_{\theta \geq 0} \psi_2(\theta) = \psi_2(\theta^*) \geq \psi_1(\theta^*) \geq \min_{\theta \geq 0} \psi_1(\theta), \quad (29)$$

which completes the proof. \square

It is noteworthy that if $M_v(\theta)$ is a monotonic increasing function of θ , we have the strict inequality in (28), i.e., \leq is replaced with $<$. In addition, an upper-bound on the outage probability of the conventional approach can be found using (27) by letting $W = \bar{W} = W_c$ as a special case.

B. Optimization and Trade-off

In this subsection, we consider an optimization problem to decide the numbers of channels for admitted UEs in the 3rd step to upload their data packets with a quality-of-service (QoS) constraint.

From (27), it can be shown that

$$\min_{\theta \geq 0} \psi(\theta; W, \bar{W}) \leq -d \Rightarrow \Pr(Q > N) \leq e^{-d}, \quad (30)$$

where $d > 0$ can be seen as the negative QoS exponent [25], [26]. For the inequality on the left-hand side (LHS) term in (30), we need the following result.

Lemma 3: Under the Poisson approximation in (22), we have

$$V \sim \text{Pois}(\lambda e^{-\frac{\lambda}{L}} \bar{s}), \quad (31)$$

where $\bar{s} = \sum_{s=1}^{s_{\max}} s\nu_s$ is the mean of the number of slots for uploading.

Proof: Since the sum of independent Poisson random variables is also Poisson, we have (31). We omit the detail as the derivation of (31) is straightforward. \square

For convenience, let $\lambda_0 = \lambda e^{-(\lambda/L)}$ and $\lambda_1 = \lambda e^{-(\lambda/L)} \bar{s}$. Then, from Lemma 3, it can be shown that

$$\begin{aligned} M_y(W\theta) &= \lambda_0(e^{W\theta} - 1), \\ M_v(\bar{W}\theta) &= \lambda_1(e^{\bar{W}\theta} - 1). \end{aligned} \quad (32)$$

From this, $\psi(\cdot)$ can be re-written as

$$\psi(\theta, W, \bar{W}) = \lambda_0 e^{W\theta} + \lambda_1 e^{\bar{W}\theta} - (\lambda_0 + \lambda_1 + N\theta). \quad (33)$$

Let $\theta(W, \bar{W})$ be the solution that minimizes $\psi(\theta, W, \bar{W})$. From (33), it can be shown that $\theta(W, \bar{W})$ is the solution of the following equation:

$$\lambda_0 W e^{W\theta} + \lambda_1 \bar{W} e^{\bar{W}\theta} = N. \quad (34)$$

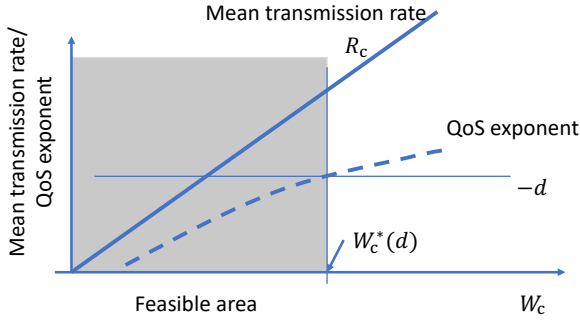


Fig. 7. An illustration of R_c and $\psi_c(\theta(W_c), W_c)$ in the conventional approach.

Since the LHS in (34) is an increasing function of θ , a sufficient condition for the existence of $\theta(W, \bar{W}) \geq 0$, which is unique, is

$$\lambda_0 W + \lambda_1 \bar{W} \leq N. \quad (35)$$

Prior to discussing the optimization of W and \bar{W} in EBT, consider the optimization for the conventional approach where $W = \bar{W} = W_c$. In this case, it can be shown that

$$\psi(\theta, W, \bar{W}) = \psi_c(\theta, W_c) \triangleq \lambda_c(e^{W_c \theta} - 1) - N\theta, \quad (36)$$

where $\lambda_c = \lambda_0 + \lambda_1$. It is trivial to show that θ minimizing $\psi_c(\theta, W_c)$ is given by

$$\theta(W_c) = \frac{1}{W_c} \ln \frac{N}{W_c \lambda_c} > 0, \text{ if } N > W_c \lambda_c. \quad (37)$$

Thus, the minimum of $\psi_c(\theta, W_c)$ becomes

$$\begin{aligned} \min_{\theta \geq 0} \psi_c(\theta; W_c) &= \psi_c(\theta(W_c), W_c) \\ &= \frac{N}{W_c} \left(1 - \ln \frac{N}{W_c \lambda_c} \right) - \lambda_c, \end{aligned} \quad (38)$$

which is an increasing function of W_c (its derivative is positive when $N > W_c \lambda_c$). Thus, for given QoS exponent d , the following rate maximization problem can be considered in the conventional approach:

$$\begin{aligned} &\max_{W_c} R_c(W_c) \\ &\text{subject to } \psi_c(\theta(W_c), W_c) \leq -d, \end{aligned} \quad (39)$$

Since R_c increases with W_c as in (3) and $\psi_c(\theta(W_c), W_c)$ is also an increasing function of W_c , the solution becomes

$$W_c^*(d) = \max \{ W_c : \psi_c(\theta(W_c), W_c) \leq -d, W_c \in \mathbb{Z}^+ \}, \quad (40)$$

where $\mathbb{Z}^+ = \{1, 2, \dots\}$ represents the set of positive integers. In Fig. 7, we illustrate R_c and $\psi_c(\theta(W_c), W_c)$, where $W_c^*(d)$ is shown to be the solution. Note that due to the fact that $\min_{\theta \geq 0} \psi_c(\theta, W_c)$ increases with W_c , by letting $W_c = 1$, we can find the following condition for the existence of a feasible solution:

$$N \left(1 - \ln \frac{N}{\lambda_c} \right) - \lambda_c \leq -d, \quad N \geq \lambda_c. \quad (41)$$

Table 1. The numbers of channels for different maximum number of slots for packet transmissions, s_{\max} , associated with Fig. 8.

s_{\max}	2	4	6	8	10	12	14	16	18	20
\bar{W}	8	7	7	7	5	8	7	6	4	3
\bar{W}	7	5	4	3	3	2	2	2	2	2
W_c	7	5	4	4	3	3	2	2	2	2

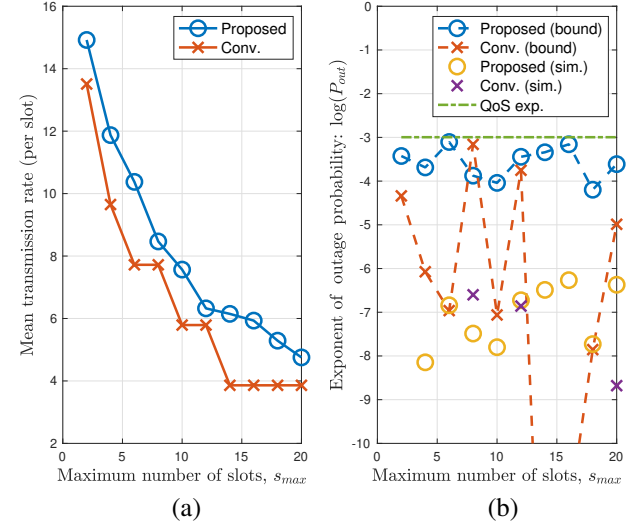


Fig. 8. Performance for different maximum number of slots for packet transmissions, s_{\max} , when $N = 200$, $\lambda = 8$, $L = 32$, and $d = -\ln(0.05)$ (i.e., $\Pr(Q > N) = 0.05$): (a) Mean transmission rate (per slot) and (b) QoS exponent.

From Fig. 7, we can also observe a trade-off relationship between the mean transmission rate, R_c , and the QoS exponent, $-d$. That is, since the mean transmission rate decreases when $-d$ decreases for a lower outage probability, it can be seen that the increase of the mean transmission rate results in a higher outage probability, vice versa.

In EBT with the QoS constraint, the rate maximization problem can be formulated as

$$\max_{W, \bar{W}} R(W, \bar{W}) \quad (42)$$

$$\text{subject to } \begin{cases} \bar{W} \leq W \\ \min_{\theta \geq 0} \psi(\theta; W, \bar{W}) \leq -d. \end{cases}$$

Clearly, if $W = \bar{W} = W_c$, the problem in (42) reduces to that in (39).

To find the optimal solution of the problem in (42), we need to have few properties as follows.

Proposition 2: For given W , consider the following sub-problem of (42):

$$\begin{aligned} &\max_{1 \leq \bar{W} \leq W} R(W, \bar{W}) \\ &\text{subject to } \psi(\theta(W, \bar{W}); W, \bar{W}) \leq -d, \end{aligned} \quad (43)$$

where

$$\theta(W, \bar{W}) = \operatorname{argmin}_{\theta \geq 0} \psi(\theta; W, \bar{W}). \quad (44)$$

Let

$$\bar{W}^*(d, W) = \max \{ \bar{W} : \psi(\theta(W, \bar{W}); W, \bar{W}) \leq -d, \bar{W} \in \mathbb{Z}^+ \}, \quad (45)$$

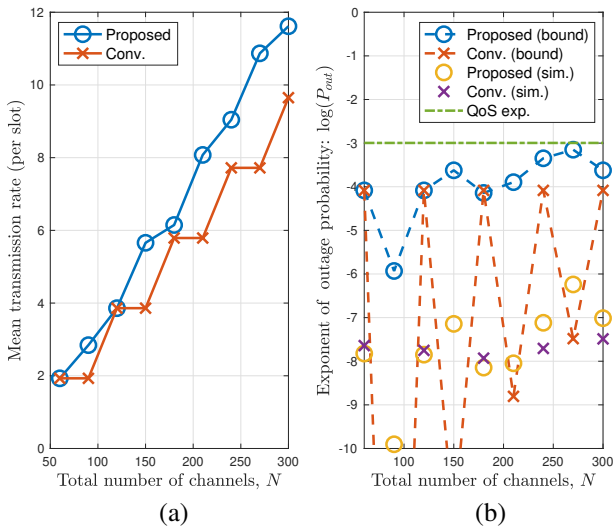


Fig. 9. Performance for different total number of channels, N , when $s_{\max} = 10$, $\lambda = 8$, $L = 32$, and $d = -\ln(0.05)$ (i.e., $\Pr(Q > N) = 0.05$): (a) Mean transmission rate (per slot) and (b) QoS exponent.

Table 2. The numbers of channels for different total number of channels, N , associated with Fig. 9.

N	60	90	120	150	180	210	240	270	300
\bar{W}	1	3	2	5	7	6	9	8	10
\bar{W}_c	1	1	2	2	2	3	3	4	4
W_c	1	1	2	2	3	3	4	4	5

which is, if exists, the optimal solution of (43).

Proof: According to Lemma 2, $\psi(\theta(W, \bar{W}); W, \bar{W})$ is an increasing function of \bar{W} (due to the strict inequality when V is Poisson). In addition, according to (2), $R(W, \bar{W})$ is an increasing function of \bar{W} for given W . As a result, for given W , if (45) has a solution for a given d , it is unique and the solution of (43). \square

Thanks to the fact that $\psi(\theta(W, \bar{W}); W, \bar{W})$ is an increasing function of \bar{W} , for given W , we can find $\bar{W}^*(d, W)$ in (45) by incrementing \bar{W} by 1 from $\bar{W} = 1$. While we can search for all W from $W = 1$ to N to find feasible $\{W, \bar{W}\}$, the following property helps reduce the search interval.

Lemma 4: Suppose that $\bar{W}^*(d, W)$ does not exist for given $W = W'$. Then, it is also true for any W'' that is greater than W' .

Since it can be easily proved by using the fact that $\psi(d, W, \bar{W})$ is also an increasing function of W , we do not provide details for the proof of Lemma 4. Note that $\min_{\theta \geq 0} \psi(\theta; W, \bar{W})$ becomes the smallest if $W = \bar{W} = 1$. Thus, in order to find any $W \geq 1, \bar{W} \geq 1$, the following condition is required:

$$\min_{\theta \geq 0} \psi(\theta; 1, 1) \leq -d, \quad (46)$$

which is equivalent to (41).

Based on the above results, in order to obtain a set of feasible pairs $\{W, \bar{W}\}$, we can have the algorithm in Algorithm 1. Once the set of feasible $\{W, \bar{W}\}$ is obtained, the optimal $\{W, \bar{W}\}$ is the pair that has the highest $R(W, \bar{W})$.

Note that the complexity of Algorithm 1 depends on the complexity of finding $\bar{W}(d, W)$ in (45). Since $\bar{W} \leq W$, for each

Algorithm 1 Finding optimal $\{W, \bar{W}\}$

Optimal: $\{W, \bar{W}\}$
Inputs: $\{\lambda_0, \lambda_1, N, d\}$
Initialization: $W = 1, \mathcal{R} = \{\}, \bar{W} = \{\}$
while $W \leq N$ **do**
 find $\bar{W}^*(d, W)$ (using Lemma 2)
 if $\bar{W}^*(d, W) \geq 1$ **then**
 $\bar{W} \leftarrow \bar{W} \cup \{\bar{W}^*(d, W)\}$
 $\mathcal{R} \leftarrow \mathcal{R} \cup \{R(W, \bar{W}^*(d, W))\}$
 $W \leftarrow W + 1$
 else
 Stop (thanks to Lemma 4)
 end
end
Output: $\{W, \bar{W}\}$ corresponding to the highest R in \mathcal{R}

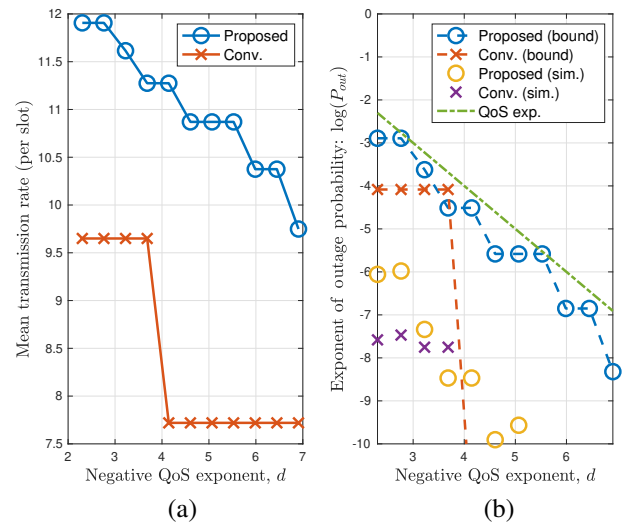


Fig. 10. Performance for different negative QoS exponent, d , when $N = 300$, $s_{\max} = 10$, $\lambda = 8$, and $L = 32$: (a) Mean transmission rate (per slot) and (b) QoS exponent.

value of $W, \bar{W} \in \{1, \dots, W\}$. Suppose that for a given pair of (\bar{W}, W) , the complexity to find $\theta(W, \bar{W})$ in (44) is Ω_0 , which is independent of W and \bar{W} . Then, the total complexity is at most $\Omega_0 \sum_{W=1}^N W = \Omega_0 N(1 + N)/2$. Furthermore, since $\psi(\theta; W, \bar{W})$ is a convex function of θ , Ω_0 depends on a numerical technique for 1-dimensional convex optimization. However, in general, Ω_0 is inversely proportional to a required precision.

In summary, to compare the overall performance of the conventional and proposed approaches, we need to find the mean rates after optimizing (W, \bar{W}) for the proposed approach via (42) and W_c for the conventional approach via (39) for given key parameters, e.g., N, λ, L , and d . Unfortunately, it is difficult to find closed-form expressions for the maximum mean transmission rates. Thus, we need to rely on numerical methods to find them, which will be considered in Section V.

V. SIMULATION RESULTS

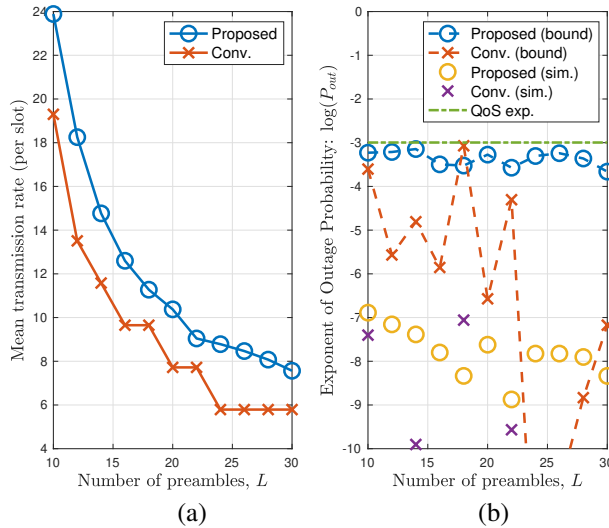
In this section, we present simulation results to see the performance of the proposed and conventional approaches with

Table 3. The numbers of channels for different negative QoS exponents, $-d$, associated with Fig. 10.

d	2.3	2.7	3.2	3.6	4.1	4.6	5.0	5.5	5.9	6.4	6.9
W	11	11	10	9	9	8	8	8	7	7	6
\bar{W}	4	4	4	4	4	4	4	4	4	4	4
W_c	5	5	5	5	4	4	4	4	4	4	4

Table 4. The numbers of channels for different numbers of preambles, L , associated with Fig. 11.

L	10	12	14	16	18	20	22	24	26	28	30
W	16	12	9	8	9	7	9	8	7	6	5
\bar{W}	9	7	6	5	4	4	3	3	3	3	3
W_c	10	7	6	5	5	4	4	3	3	3	3

Fig. 11. Performance for different numbers of preambles, L , when $N = 300$, $s_{\max} = 10$, $\lambda = 20$, and $d = -\ln(0.05)$ (i.e., $\Pr(Q > N) = 0.05$): (a) Mean transmission rate (per slot) and (b) QoS exponent.

$\{W, \bar{W}\}$ and W_c by solving (39) and (42) under the assumption of independent Rayleigh fading channels in (4). For convenience, we assume that $\bar{\gamma} = 6$ dB for all UEs. Furthermore, independent Poisson arrivals are assumed for the UEs that send randomly selected preambles from a pool of L preambles with mean arrival rate λ . For the number of slots for packet transmissions, s , is assumed to have a uniform distribution so that $\nu_s = 1/s_{\max}$, $s = 1, \dots, s_{\max}$.

In Fig. 8, we show the performance for different maximum numbers of slots for packet transmissions, s_{\max} , in terms of the mean transmission rate and QoS exponent when $N = 200$, $\lambda = 8$, $L = 32$, and $d = -\ln(0.05)$ (i.e., $\Pr(Q > N) \leq 0.05$). In addition, the corresponding optimal numbers of channels for exploration and exploitation (i.e., W and \bar{W} , respectively) are shown together with W_c in Table 1. It is shown that the mean transmission rate per slot, $R(W, \bar{W})$, of EBT is higher than that of the conventional approach, $R_c(W_c)$, for a wide range of s_{\max} , while all the QoS exponents are less than $-d \approx 2.9957$ (or $\Pr(Q > N) = 0.05$). We also see that the number of channels per UE (i.e., W and \bar{W} in EBT and W_c in the conventional approach) decreases with s_{\max} in Table 1, which also results in the decrease of the mean transmission rate as shown in Fig. 8. This is expected as there are more packets to be transmitted from UEs with a larger s_{\max} .

The impact of the total number of channels, N , on the per-

formance is illustrated in Fig. 9 when $s_{\max} = 10$, $\lambda = 8$, $L = 32$, and $d = -\ln(0.05)$ (i.e., $\Pr(Q > N) = 0.05$). As shown in Fig. 9, the increase of N results in the increase of the mean transmission rate with keeping the QoS exponent lower than $-d$. Clearly, the increase of the mean transmission rate can be achieved by increasing W and \bar{W} in EBT and W_c in the conventional approach as shown in Table 2. It is interesting to see a particular case that $N = 300$. According to Table 2, the optimal numbers of channels for exploration and exploitation in EBT are $W = 10$ and $\bar{W} = 4$, respectively, while W_c in the conventional approach is 5. Since $s_{\max} = 10$, we have $\bar{s} = 5.5$. On average, each UE in the conventional approach sends a total of $(\bar{s} + 1)W_c = 6.5 \times 5 = 32.5$ packets⁴. On the other hand, in EBT, each UE sends a total of $W + \bar{s}\bar{W} = 10 + 5.5 \times 4 = 32$ packets on average. That is, the numbers of transmitted packets in both the approaches are almost the same. In this case, while their QoS exponents are comparable, we can see that the mean transmission of EBT is higher than that of the conventional approach as shown in Fig. 9.

As discussed earlier, the optimal numbers of channels can be found by solving (39) and (42) for a given QoS exponent. In Fig. 10, we show the performance for different negative QoS exponent, d , when $N = 300$, $s_{\max} = 10$, $\lambda = 8$, and $L = 32$. As shown in Fig. 10(b), it is possible to keep the upper-bound on the QoS exponent below $-d$ by choosing optimal W and \bar{W} in EBT. We see that the mean transmission rate of EBT is higher than that of the conventional approach for any value of d .

In Table 3, we can see the optimal numbers of channels for each UE associated with Fig. 10. There are two variables, W and \bar{W} , for the optimization in EBT, while there is only one variable, W_c , in the conventional approach. Consequently, it is possible to jointly optimize the pair of W and \bar{W} so that the resulting QoS exponent is sufficiently close to $-d$ in EBT. However, in the conventional approach, the optimization result is coarse as there is only one variable, i.e., $W_c \in \{1, 2, \dots\}$, to be optimized, which results in a QoS exponent that is a bit loose. For example, when $d = -\ln(0.01) \approx 4.6$, the optimal number of channels in the conventional approach is $W_c = 4$. However, with $W_c = 5$, it results in $d = 4.083$, which is slightly lower than the target negative QoS exponent, $d = 4.6$. From this, we can see that another salient advantage of EBT over the conventional one is that the radio RBs can be more precisely allocated to meet a QoS requirement thanks to an additional variable in terms of optimization perspective.

In Fig. 11, we show the performance for different numbers of preambles, L , when $N = 300$, $s_{\max} = 10$, $\lambda = 20$, and $d = -\ln(0.05)$. Since λ is fixed, as L increases, there are less preamble collisions, which leads to more admitted UEs per slot in the third step. As a result, we can see that the mean transmission rate decreases with L , while the QoS exponents are all less than $-d$ due to optimal allocation of channels per UE (as shown in Fig. 11 (b)). It is also observed that the numbers of channels per UE, W and \bar{W} , in EBT decrease with L , which is also true in the conventional approach as shown in Table 3.

According to Figs. 8(b)–11(b), it has been observed that the actual QoS exponents obtained by simulations are lower than the

⁴It includes pilot signals transmitted by a UE to allow the BS to estimate the channel coefficients and SNR.

QoS exponents that are obtained from the theory (e.g., (38) for the conventional approach). The gap is due to a number of reasons as follows: *i*) The Poisson approximation in (21) and (22); *ii*) the Chernoff bound in (24). In particular, since Z in (20) is a binomial variable, Z cannot be larger than L . However, in (21), due to the Poisson approximation, Z can be larger than L , which results in a heavier tail probability of Q than the actual one and a loose upper-bound in (24). Thus, we need to consider different methods to find tighter bounds as a further research topic. Other further research topics are to be discussed in Section VI.

VI. CONCLUDING REMARKS

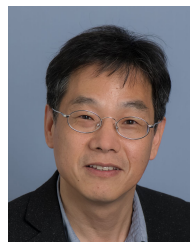
In this paper, we proposed EBT that can increase the mean transmission rate by exploiting the multichannel selection diversity gain for uplink transmissions in MTC. To exploit the channel selection diversity gain, in particular, a BS initially allocated W channels to a new admitted UE in the third step and estimated their SNRs. Then, the BS sent the indices of the best \bar{W} channels so that the UE can use them to upload their data packets, where $\bar{W} < W$. In general, for a fixed \bar{W} , it was shown that a higher multichannel selection diversity gain can be achieved as W increases. Compared with the conventional approach where $W = \bar{W} = W_c$, it was shown that EBT can have an improved transmission rate. However, since the use of more channels for exploration can result in a higher outage probability, an optimization problem was formulated with an outage probability constraint to allow a fair comparison with the conventional approach from a multiuser system point of view. We also derived an algorithm to find the optimal numbers of channels for exploration and exploitation, i.e., W and \bar{W} , in EBT. From simulation results, we confirmed that EBT can provide a higher mean transmission rate than the conventional one under various conditions thanks to multichannel selection diversity.

There are a number of issues to be studied in the future. Firstly, time-varying channels need to be studied, while we only focus on static channels in this paper. In particular, for mobile UEs, it is necessary to generalize the channel selection to take into account time-varying channels. Second, a more realistic objective function (instead of mean transmission rate) can be considered with finite-length codes and re-transmission protocols (e.g., hybrid automatic repeat request (HARQ) protocols [27], [28]). Third, as mentioned earlier, it is interesting to find a tighter upper-bound on the outage probability as the Chernoff bound with Poisson approximation turns to be a bit loose.

REFERENCES

- [1] J. Ding, M. Nemati, C. Ranaweera, and J. Choi, "IoT connectivity technologies and applications: A survey," *IEEE Access*, vol. 8, pp. 67646–67673, April 2020.
- [2] B. K. J. Al-Shammari, N. Al-Aboody, and H. S. Al-Raweshidy, "IoT traffic management and integration in the QoS supported network," *IEEE Internet Things J.*, vol. 5, no. 1, pp. 352–370, Feb. 2018.
- [3] 3GPP TR 37.868 V11.0, *Study on RAN improvements for machine-type communications*, Oct. 2011.
- [4] J. Park, S. Samarakoon, M. Bennis, and M. Debbah, "Wireless network intelligence at the edge," *Proc. IEEE*, vol. 107, no. 11, pp. 2204–2239, Nov. 2019.
- [5] 3rd Generation Partnership Project (3GPP), *Evolved Universal Terrestrial Radio Access (EUTRA) and Evolved Universal Terrestrial Radio Access Network (EUTRAN); Overall Description, TS 36.300 v.14.7.0*, June 2018.

- [6] T. Kwon and J.-W. Choi, "Multi-group random access resource allocation for M2M devices in multicell systems," *IEEE Commun. Lett.*, vol. 16, no. 6, pp. 834–837, June 2012.
- [7] E. Paolini, C. Stefanovic, G. Liva, and P. Popovski, "Coded random access: applying codes on graphs to design random access protocols," *IEEE Commun. Mag.*, vol. 53, no. 6, pp. 144–150, June 2015.
- [8] J. Choi, "NOMA-based random access with multichannel ALOHA," *IEEE J. Sel. Areas Commun.*, vol. 35, no. 12, pp. 2736–2743, Dec. 2017.
- [9] C. Bockelmann *et al.*, "Massive machine-type communications in 5G: Physical and MAC-layer solutions," *IEEE Commun. Mag.*, vol. 54, no. 9, pp. 59–65, Sept. 2016.
- [10] Ericsson, "Cellular IoT evolution for industry digitalization," *White Paper*, Jan. 2019.
- [11] Y. Song, K. W. Sung, and Y. Han, "Coexistence of Wi-Fi and cellular with listen-before-talk in unlicensed spectrum," *IEEE Commun. Lett.*, vol. 20, no. 1, pp. 161–164, Jan. 2016.
- [12] H. B. Rekhissa, C. Belleudy, and P. Bessagnet, "Energy efficient resource allocation for M2M devices in LTE/LTE-A," *Sensors*, vol. 19, no. 24, p. 5337, Dec. 2019.
- [13] J.-B. Seo, H. Jin, and B. C. Jung, "Multichannel uplink NOMA random access: Selection diversity and bistability," *IEEE Commun. Lett.*, vol. 23, no. 9, pp. 1515–1519, June 2019.
- [14] Y. Chen, S. Li, C. Li, Y. T. Hou, and B. Jalaian, "To cancel or not to cancel: Exploiting interference signal strength in the eigenspace for efficient MIMO DoF utilization," *Proc. IEEE INFOCOM*, May 2019.
- [15] J. Choi, "Two-stage multiple access for many devices of unique identifications over frequency-selective fading channels," *IEEE Internet Things J.*, vol. 4, no. 1, pp. 162–171, Feb. 2017.
- [16] A. T. Abebe and C. G. Kang, "Comprehensive grant-free random access for massive low latency communication," in *Proc. IEEE ICC*, May 2017.
- [17] C. Bockelmann *et al.*, "Towards massive connectivity support for scalable mMTC communications in 5G networks," *IEEE Access*, vol. 6, pp. 28969–28992, May 2018.
- [18] J. Choi, "On throughput of compressive random access for one short message delivery in IoT," *IEEE Internet Things J.*, vol. 7, no. 4, pp. 3499–3508, April 2020.
- [19] 3GPP TS 36.321 V13.2.0, *Evolved Universal Terrestrial Radio Access (E-UTRA); Medium Access Control (MAC) protocol specification*, June 2016.
- [20] H. S. Jang, S. M. Kim, H. Park, and D. K. Sung, "An early preamble collision detection scheme based on tagged preambles for cellular M2M random access," *IEEE Trans. Veh. Technol.*, vol. 66, no. 7, pp. 5974–5984, July 2017.
- [21] H. A. David and H. N. Nagaraja, *Order Statistics*. New York: John Wiley & Sons, third ed., 2003.
- [22] T. M. Cover and J. A. Thomas, *Elements of Information Theory*. NJ: John Wiley, second ed., 2006.
- [23] M.-S. Alouini and A. J. Goldsmith, "Capacity of Rayleigh fading channels under different adaptive transmission and diversity-combining techniques," *IEEE Trans. Veh. Technol.*, vol. 48, no. 4, pp. 1165–1181, July 1999.
- [24] M. Mitzenmacher and E. Upfal, *Probability and Computing: Randomized Algorithms and Probability Analysis*. Cambridge University Press, 2005.
- [25] F. Kelly and E. Yudovina, *Stochastic Networks*. Cambridge University Press, 2014.
- [26] C.-S. Chang and J. A. Thomas, "Effective bandwidth in high-speed digital networks," *IEEE J. Sel. Areas Commun.*, vol. 13, no. 6, pp. 1091–1100, Aug. 1995.
- [27] S. B. Wicker, *Error Control Systems for Digital Communication and Storage*. Prentice Hall, 1995.
- [28] S. Lin and D. J. Costello, Jr., *Error Control Coding: Fundamentals and Applications*. Englewood Cliffs, N.J.: Prentice Hall, 1983.



Jinho Choi (SM'02) was born in Seoul, Korea. He received B.E. (magna cum laude) degree in Electronics Engineering in 1989 from Sogang University, Seoul, and M.S.E. and Ph.D. degrees in Electrical Engineering from Korea Advanced Institute of Science and Technology (KAIST) in 1991 and 1994, respectively. He is with the School of Information Technology, Burwood, Deakin University, Australia, as a Professor. Prior to joining Deakin in 2018, he was with Swansea University, United Kingdom, as a Professor/Chair in Wireless, and Gwangju Institute of Science and Technology (GIST), Korea, as a Professor. His research interests include the Internet of things (IoT), wireless communications, and statistical signal processing. He

authored two books published by Cambridge University Press in 2006 and 2010. Prof. Choi received the 1999 Best Paper Award for Signal Processing from EURASIP, 2009 Best Paper Award from WPMC (Conference), and is Senior Member of IEEE. Currently, he is an Editor of IEEE Trans. Communications and IEEE Wireless Communications Letters and a Division Editor of Journal of Communications and Networks (JCN). He also had served as an Associate Editor or Editor of other journals including IEEE Communications Letters, JCN, IEEE Trans. Vehicular Technology, and ETRI journal.



Jihong Park (S'09-M'16) is a Lecturer at the School of IT, Deakin University, Australia. He received the B.S. and Ph.D. degrees from Yonsei University, Seoul, Korea, in 2009 and 2016, respectively. He was a Post-Doctoral Researcher with Aalborg University, Denmark, from 2016 to 2017; the University of Oulu, Finland, from 2018 to 2019. His recent research focus includes communication-efficient distributed machine learning, distributed control, and distributed ledger technology, as well as their applications for beyond 5G/6G communication systems. He served as a Conference/Workshop Program Committee Member for IEEE GLOBECOM, ICC, and INFOCOM, as well as NeurIPS, ICML, and IJCAI. He received the IEEE GLOBECOM Student Travel Grant in 2014, the IEEE Seoul Section Student Paper Contest Bronze Prize in 2014, and the 6th IDIS-ETNEWS (The Electronic Times) Paper Contest Award sponsored by the Ministry of Science, ICT, and Future Planning of Korea. Currently, he is an Associate Editor of Frontiers in Data Science for Communications, a Review Editor of Frontiers in Aerial and Space Networks, and a Guest Editor of MDPI Telecom SI on "millimeter wave communications and networking in 5G and beyond."



Shiva Raj Pokhrel(M'19) is a Lecturer of Mobile Computing at Deakin University, Geelong, Australia. He received the B.E./M.E. degree in 2007/2013 from Pokhara University, Nepal and Ph.D. degree in 2017 from Swinburne University of Technology, Australia. He was a Research Fellow at the University of Melbourne and a Network Engineer at Nepal Telecom (2007-2014). His research interests include multi-connectivity, federated learning, industry 4.0 automation, blockchain modeling, optimization, recommender systems, 6G, cloud computing, dynamics control, Internet of Things and cyber-physical systems as well as their applications in smart manufacturing, autonomous vehicles and cities. He was a recipient of the prestigious Marie Skłodowska-Curie grant Fellowship in 2017.